Online ISSN 1848-3380, Print ISSN 0005-1144
ATKAFF 53(2), 142–155(2012)

Doron Shmilovitz, Yoash Levron

Distributed Maximum Power Point Tracking in Photovoltaic Systems – Emerging Architectures and Control Methods

DOI 10.7305/automatika.53-2.185
UDK 621.383.51
IFAC 4.2; 4.3.2.4

Original scientific paper

The interest in distributed maximum power point tracking increases along with increasing deployment of photovoltaic generators and the constant pressure to reduce the cost of photovoltaic generated energy. Distributed maximum point tracking facilitates a significant boost of captured photovoltaic power.

In this paper we compare different distributed maximum power point architectures, and categorize them into two main groups; those which process the entire generated power and partial power processing based architectures. The first ones are found to be easier to control while the second ones exhibit higher efficiency. Some delicate control issues are emphasized; a distinction is made between maximum power point tracking and negative feedback control. For systems consisting of multiple power processors, we derive the required number of maximum point tracking units and their adequate location within a global architecture. Only the right number of units guarantees extraction of the entire potential power as well as system stability. In contrary, we demonstrate how instability occurs due to a redundant control structure.

Key words: Maximum power point tracking (MPPT), Module integrated converter (MIC), DC optimizer, Distributed maximum power point tracking (DMPPT)

Distribuirano praćenje točke maksimalne snage u fotonaponskim sustavima – nove arhitekture i metode upravljanja. Interes za distribuirano praćenje točke maksimalne snage se povećava zajedno sa rastućim razvojem fotonaponskih sustava i konstantnim pritiskom da se smanji cijena energije iz fotonaponskih sustava. Distribuirano praćenje točke maksimalne snage omogućava značajan porast dobivene fotonaponske snage.

U ovom članku uspoređene su različite arhitekture distribuirane točke maksimalne snage, te su kategorizirane u dvije glavne skupine; one koje procesiraju čitavu generiranu snagu i one temeljene na parcijalnom procesiranju snage. Pokazuje se da je prva skupina jednostavnija za upravljanje, dok je druga skupina efikasnija. Naglasak je stavljena na određena osjetljiva pitanja vezana za upravljanje; razlučuje se praćenje točke maksimalne snage i negativna povratna veza. Za sustave koji se sastoje od više procesora snage, izveden je potreban broj jedinica za praćenje maksimalne točke, te njihova adekvatna lokacija u globalnoj arhitekturi. Samo ispravan broj jedinica osigurava dobivanje čitave potencijalne snage kao i stabilnost sustava. S druge strane, pokazano je kako uslijed redundantne upravljačke strukture dolazi do nestabilnosti.

Ključne riječi: praćenje točke maksimalne snage (MPPT), pretvarač integriran na modulu (MIC), DC optimizator, distribuirano praćenje točke maksimalne snage (DMPPT)

1 INTRODUCTION

Typically, in photovoltaic (PV) systems a high voltage is obtained by connecting multiple modules in series to form a string of modules. Since modules in a string are connected in series, a mismatch of currents among the individual modules reduces the output current of the whole string, inserting losses which are disproportional to the shading. In attempting to address this problem, module level maximum power point tracking (MPPT) methods, otherwise known as distributed maximum power point tracking (DMPPT), are increasingly reported. In some architectures, auxiliary power processors are inserted in cascade (in the main power-flow path). These architectures are referred to as 'full power processing MPPT'. In other architectures, the auxiliary processors are used just for balancing the PV string, while most of the string's power flows directly without additional processing. These architectures are referred to as 'minimal power processing MPPT'.

Various full power processing architectures have been suggested. The inherent split source nature of PV generators may be employed beneficially. For instance the power may be processed by modular converters or by a multi-

level inverter. In addition, assuming split power processing, each individual module may be optimized to provide maximum power. For instance, it is stated in [1] that front end DMPPT can result in up to 25% increase of overall power. The relatively old concept of a module integrated inverter is nowadays known as micro inverter and gains renewed interest [2, 3]. Recently, many works reported efforts to maximize the extracted power on the DC side [4-7]. Walker et al. introduced 'distributed power conditioning' (later known as distributed MPPT—DMPPT), where MPP tracking is performed at the module level by means of module integrated DC-DC converters (MIC), located at each PV module's front end [4]. In these architectures, the converters' outputs are typically connected in series to form a string. The MIC-based DMPPT concept was further investigated to derive the small-signal AC model and to analyze its steady-state behavior, dynamics and stability, as well as aspects concerning the converter association [6]. While it was concluded in [1] that front end DMPPT can result in power capture increase compared to standard MPPT (depending on the standard deviation in incident light), it was also pointed out that under near-uniform lighting conditions, the benefits of DMPPT can be outweighed by losses in the MICs.

A research effort combining an analysis of shading patterns and distributed power electronic converters of various granularity attempted to quantify the benefits of DMPPT [8]. It was concluded in this paper that in two out of three installations, the energy yield benefit outweighs the power electronics costs and that panel and sub-string-level DMPPT seem to be the appropriate levels of granularity.

Among the various ways to implement the MIC's power stage, [4, 7, 8], the bridge based buck/boost topology seems most adequate due to the high efficiency it exhibits over a wide power range, its buck, boost, and pass-through capabilities, and its relatively low-cost [9, 10]. The optimization of the bridge based buck/boost topology for efficiency and control of an individual MIC were detailed in [10, 11]. Due to the extreme gain that MICs might be required to provide in highly mismatched situations, the performance degrades even with the MIC-based DMPPT architecture. In order to overcome this shortcoming, [12] proposed augmenting MIC-based DMPPT architecture by a string current diverter that decouples MIC corresponding to the shaded Module from the rest of the string.

The advantages of source splitting, i.e, input ports supplied by independent modules, were recognized in an even earlier paper - [13], where N PV modules (N=4) were interfaced by buck-boost DC-DC converters, which exhibit loss free resistor characteristics. The converters' outputs were connected in parallel across the inverter input where the power of all N channels accumulated.

The potential advantage of such a modular system was addressed in this paper, particularly in the case of inhomogeneous insolation. However, the series-connection of the MICs output ports, as in [4-7], provides the high voltage required for DC-AC conversion and facilitates a higher overall conversion efficiency. In similarity to [13, 14] proposed the parallel connection in the context of building integrated PV. There, each module was coupled to a high voltage (200V/400V) dc bus through a dc-dc converter (thus the MICs are connected in parallel at their outputs). Then, a central inverter was fed from the dc bus, where the power of all modules accumulated. In order to attain a high gain and yet high efficiency, a transformer based current-fed half-bridge converter was employed in this architecture [15].

Another interesting approach to overcome mismatch losses was reported in [16, 17]; reconfiguring the modules interconnection throughout the day resulted in 3%-5% increased energy harvest. Recently proposed active bypass diodes represents another form of distributed power processing on the DC side of PV strings [18, 19]. Under this method, conducting bypass diodes are shunted by and active switch (such as MOSFET or BJT) thus reducing the voltage drop across the bypass from the diode forward voltage to the saturation voltage of a BJT. According to [18] this could manifest in up to 1% increased power capture at maximum power point.

Another DMPPT approach, the 'minimal power processing', applies DC-DC converters just for balancing the PV string, while most of the string's power flows directly without being processed by the converters [20-25], thus the losses are reduced considerably.

In this paper we review DC side DMPPT architectures and compare them with respect to their operation principles and performance. Full power processing architectures are compared to those with minimal power processing. The first architectures are found to be easier to control while the second ones exhibit higher efficiency.

Some delicate control issues are emphasized; a distinction is made between maximum power point tracking and negative feedback control. For systems consisting of multiple power processors, we derive the required number of maximum point tracking units and their adequate location within a global architecture. Only the right number of units guarantees extraction of the entire potential power as well as system stability. In contrast, we demonstrate how instability occurs due to a redundant control structure.

2 PHOTO VOLTAIC MISMATCH MECHANISMS

Mismatch among PV modules may occur due to differences in temperature, insolation, manufacturing tolerance, aging, etc. Regardless of the cause of the mismatch, this situation manifests as an asymmetry in the current-voltage

$(i-v)$ characteristics of PV modules. Thus, since some of the PV modules within a PV string exhibit different $i-v$ characteristics from others, it is impossible to find an operation point at which all the modules in the string operate at the maximum power point (MPP).

The operation of PV strings under uneven insolation and the mismatch losses origin and impact are discussed in this section. The well-known single-diode PV cell model is shown in [26, 27]. It consists of a photon generated current source whose magnitude is proportional to the insolation, a diode, a series resistance, r_s, and a shunt resistance R_{sh}. Since R_{sh} is very high and r_s is very low, without loss of generality these elements are neglected resulting in the simplified PV cell model shown in Fig. 1(b). This simplified model exhibits $i-v$ characteristics which are sharper than the actual PV cell's characteristics (rather square shape), i.e. this model implies a quality factor which is higher than that of the actual cell. Nevertheless, the critical PV cell's parameters influencing the following derivation, such as open circuit voltage, short circuit current, and v_M – the voltage at the point of maximum power, are pretty much preserved. More importantly, the operation modes are preserved. Thus we employ the reduced model of Fig. 1(b) in our analysis. Consider a substring of PV cells connected in series (note later on a substring is determined by having at most one bypass diode across it). Applying the cell model depicted in Fig. 1(b), a substring composed of n PV cells may be modeled as in Fig. 2(a).

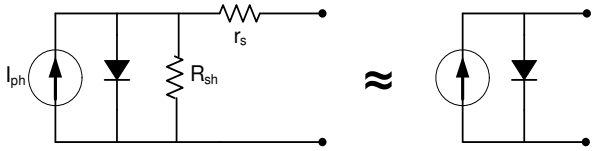

Fig. 1. (a) The single-diode cell model, (b) Simplified cell model

One may assume that, to some extent, the photo currents of the cells within a substring have close magnitudes one to the other. This is not necessarily always so, however the discussion herein is restricted to the substring granularity. Thus, assuming uniform insolation across the substring, the current sources in Fig. 2(a) are all equal and the substring may be modeled by a single current source in parallel with n diodes as shown in Fig. 2(b). Let us consider now a string of N PV modules as in Fig. 3(a) which may be modeled by means of the substring model of Fig. 2(b). Note that, for the sake of simplicity, we assume that each module consists of a single substring. Suppose the k^{th} module is shaded to a certain degree - $\%shade$. This would

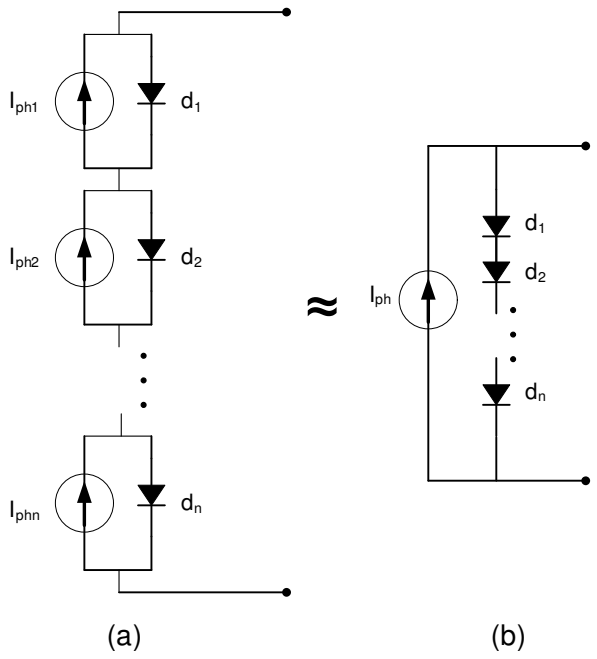

Fig. 2. (a) String of cells, (b) Single current source string model, assuming homogenous insolation

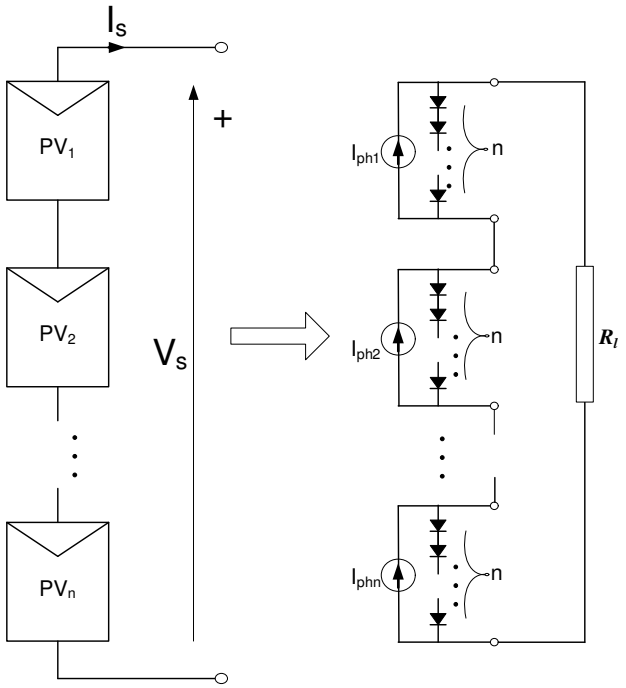

Fig. 3. (a) String of PV modules, (b) The string modeled by the single current source model

result in a proportionally reduced photo-generated current:

$$\begin{aligned} I_{ph-k} &= \alpha I_{nom}, \\ I_{ph-j,j\neq k} &= I_{nom}, \end{aligned} \tag{1}$$

where $\alpha = 1 - \%shade$ and I_{nom} is the photon generated current of the rest (non shaded) modules in the string. Clearly the shaded module limits the entire string's current. Swiping the string's load from $R_l = 0$ to $R_l = \infty$, yields Fig. 4. This simulation was carried out for a 5 module string (N=5). The module's main parameters are: V_m, I_M, P_M, V_{oc} and I_{sc}. One of the modules was assumed to be 62.5% shaded, i.e. $\alpha = 0.375$.

This PSPICE simulation clearly demonstrates the detrimental effects of mismatch:

a Since the shaded module limits the entire string current, as may be seen in Fig. 4(a), the losses are actually magnified by N. The string maximum power is approximately $P_{M\_string} = \alpha \cdot P_M$, see Fig. 4(b). However, only one module is shaded, thus the potential string power is much higher:

$$P_{pot} = (N - 1 + \alpha) \cdot P_M \tag{2}$$

b At a string voltage of approximately $V_S = (N-1) \cdot V_{OC}$, the shaded module's voltage reverses and the module starts consuming power, see Fig. 4(c) and (d). At low string voltages, the reverse voltage across the shaded module may approach $v_k \to (N-1) \cdot V_{OC}$. In long strings, the reverse voltage across the shaded module may reach the cells breakdown voltage and the power dissipation may cause hot spots. In both cases the PV cells may be permanently damaged.

In order to prevent the above detrimental situations, bypass diodes are normally incorporated in shunt with the PV modules (or substrings of cells). These diodes become forward biased whenever a module generates less current than the rest of the modules in the string. Thus these diodes protect the modules/cells against reverse high voltages and also prevent hot spots.

Moreover, since the diode conducts the string current, the 'weak' module no longer limits the string's current and more power may be extracted.

Unfortunately, the bypass-diodes protected string also presents some shortcomings. The string's $i - v$ characteristics exhibit a step-like shape due to the bypass diodes, which manifests as a multi peak power curve. This poses a difficulty for the MPPT unit (to identify the absolute maximum). Moreover, the bypassed module (or substring) potential power is lost due to being bypassed.

3 DISTRIBUTED MAXIMUM POWER POINT TRACKING ARCHITECTURES

With the increasing deployment of PV generation and the constant need to reduce the cost of PV generated electricity, mismatch losses can no longer be tolerated. This gave rise to a new group of PV architectures, called Distributed Maximum Power Point Tracking (DMPPT). DMPPT facilitates the extraction of maximum power from each individual module, thus eliminating the mismatch losses. Three DMPPT architectures are shown in Fig. 5. Micro-inverters (Fig. 5(a)) supply the PV generated power directly to the power grid. The second class DMPPT employs Front-end DC optimizers (Fig. 5(b)), also known as Module Integrated Converters (MICs). The MICs are connected in front of the PV modules and their outputs are connected in series to form a string. In this architecture, the MPPT is performed on a per-module basis, thereby allowing PV modules to operate at different currents – each module at its MPP current. Thus, underperforming modules do not limit the whole string, nor are they bypassed. Each module contributes its entire potential power.

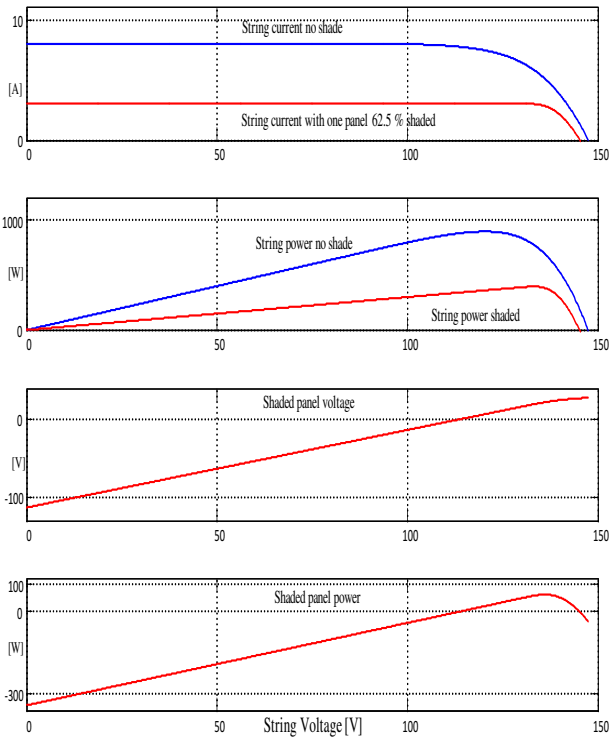

Fig. 4. Characteristics of a five module string where one module is 62.5% shaded (a) string current with and without shade, (b) string power with and without shade, (c) shaded module voltage, and (d) shaded module power

The micro-inverters and front-end DC optimizers are 'full power processing' architectures, meaning that each converter processes the entire power generated by its associated PV module regardless of shading conditions. In a third DMPPT architecture class, referred to as 'Minimal power processing' architectures, only a small fraction of

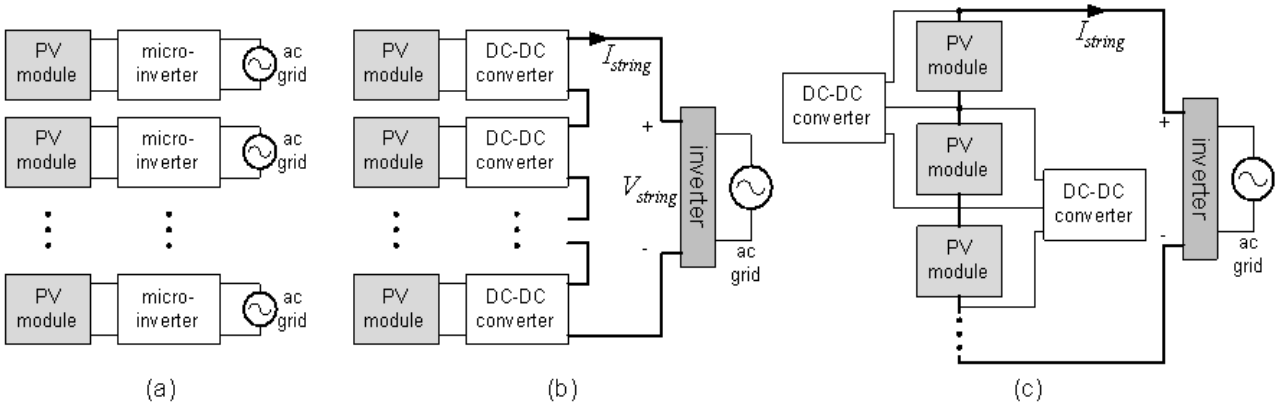

Fig. 5. Distributed maximum point tracking architectures (a) micro-inverters, (b) front-end DC optimizers, and (c) minimal power-processing: shuffling architecture

the generated power is processed by the DC-DC converters in order to just balance the modules operation point [7, 20-25]. The shuffling DC optimizers' scheme [20], shown in Fig. 5(c), is a representative example of this category. Mismatch losses occur when the currents generated by the PV modules are unequal. These losses can be avoided, provided the symmetry among the modules is restored. The shuffling topology balances the PV generated currents, and restores the symmetry of the string.

This is accomplished by DC-DC converters applied in parallel with each PV module pair, as shown in Fig. 5(c). The converters' outputs can be viewed as shunt current sources that complement the photon-generated current of shaded modules. These converters inject across the module the right amount of current to match it to the adjacent one. Thus, the joint currents of all module-converter pairs in a string are equalized. Once the currents are matched, mismatch losses are eliminated and the entire potential energy of the PV system can be extracted towards the load.

Contrary to the full power architectures, minimal power architectures process just a small portion of the overall power. Most of current flows directly through the PV string, without being processed by the converters. Comparing to full power architectures, minimal-power architectures result in three major advantages: reduced converters' rating, converter operation under lower stress, and much lower losses. However, the MPPT algorithm and the wiring are more complex.

4 FRONT END DC OPTIMIZERS

Front end DC optimizers are usually efficient, simple, and economical, thus they attract academic research and are also becoming popular in industry [4-11, 14, 15]. In principle, the converters are embedded within the PV module, hence named 'Module Integrated Converters' (MICs). The maximum power point of each PV module is tracked locally by its associated converter, and is unaffected by the string. As a result, energy harvest can potentially increase by 30%-45% in comparison to traditional string architectures [7]. In addition, the integrated units facilitate secondary features, such as status monitoring of individual modules, security protection (such as anti-theft) and safety features (such as 'electronic switch off' to prevent electrification and arcing hazards on the dc side), internet connection, and so forth.

There are many ways to implement the MIC's power stage [7, 8]. Recently, the bridge based buck/boost topology, depicted in Fig. 6, became popular due to the high efficiency it exhibits over a wide range of voltage gains, its buck and boost (and pass-through) capability, and its low-cost [5, 7, 11]. This power stage utilizes four switches: N1 - N4, and can operate in either one of three modes: buck,

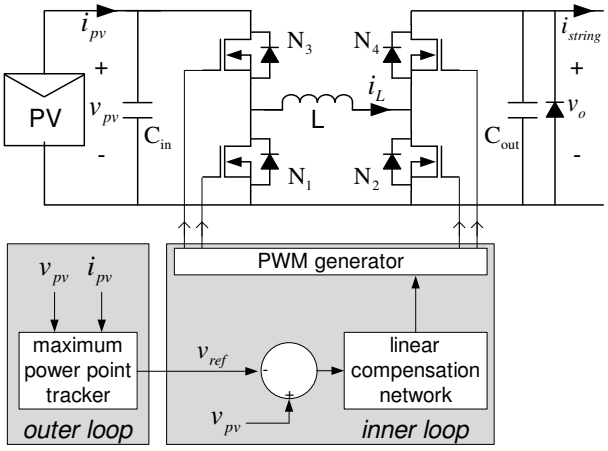

Fig. 6. Bridge based buck/boost topology

boost, or pass-through. The buck mode is selected whenever the input voltage, v_{pv}, is higher than the output voltage, v_o. In this mode, switch N4 is constantly closed, and switch N2 is constantly open. Switches N1 and N3 are supplied with a nearly complementary (with proper dead time to prevent shoot- through conduction) PWM command, thus implementing a synchronous buck. The boost mode is entered when the output voltage is higher than the input.

In this mode, N3 is closed, N1 is open, and N2, N4 implement the synchronous boost by switching on and off periodically (complementary with certain dead time).

A third mode, the pass-through mode, is selected when the output and input voltages are close to one another, so the MIC's required gain is close to unity. In this mode, N3, N4 are closed, and N1, N2 are open. No switching occurs (and no switching losses) consequently the efficiency is very high [7].

4.1 DC Optimizers Control

MICs are typically controlled locally and independently from one another. Each converter tracks the MPP of its module autonomously applying a dual loop control scheme, as shown in Fig. 7. A slow outer MPPT scheme generates a reference signal (mostly an input voltage reference) which is fed to a high bandwidth inner loop. The inner loop typically consists of a linear control network, implementing regulation of the input voltage by means of feedback.

Thus the inner loop regulates the operation point of the PV module, stabilizing it against transients of string current, while the outer loop slowly adjusts the operation point to match variations of insolation and other atmospheric conditions. Thus, while the inner feedback loop can be implemented either digitally or by a simple analogue circuitry, the outer loop realizes an iterative search

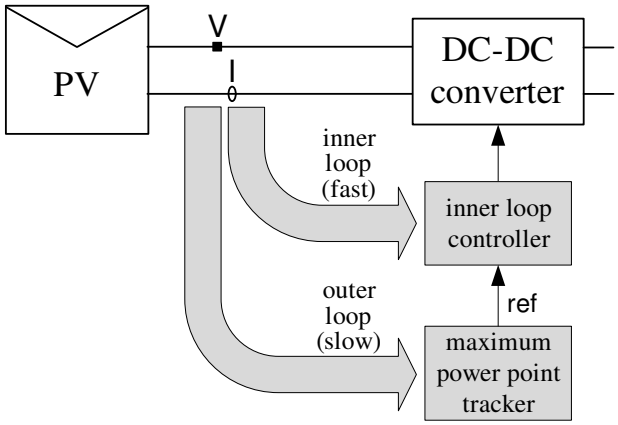

Fig. 7. Dual-loop MPPT

of the MPP, which relies on a microcontroller implemented MPPT algorithm [7, 11]. In this scheme, the converters' dynamics are decoupled from the tracking of maximum power.

The string output voltage is regulated by the inverter. It is chosen to be somewhat higher than the AC voltage peak in order to allow efficient power conversion without exposing the power MOSFETs to a high voltage stress. The DC-DC converters automatically adjust their gains to match the string's voltage. The number of PV modules in a string is typically chosen so that the required converter's gain will be close to unity. As a result, under nominal insolation, most of the converters can operate in the 'pass-through' mode, reducing the amount of switching and increasing the overall efficiency.

The abrupt transition from one operation mode to another (buck / pass-through / boost) is challenging and has been the focus of a few recent works [11, 28-30]. With conventional PWM controllers, the transition to and from the pass-through mode can provoke high voltage transients and increased ripple because it is associated with an abrupt change of the effective switching frequency, which is constant in the buck or the boost modes and zero in the pass-through-mode. In addition, due to limitations such as modulator saturation (or minimum on or off times of digital controllers) unity gain can be approached only to a certain limit by the buck or the boost topologies [10, 11].

4.2 Location of the MPPT Units

The position of the MPPT units seems intuitive, yet in some designs might be confusing as it is not always clear whether an MPPT unit or a simple closed-loop regulator should be applied. Recall the difference between the two: MPPT units implement active iterative algorithms, searching for an optimal operation point, while closed-loop regulators just fix the voltage or current to a given reference, applying negative feedback, (mostly applying linear control).

In [31] a theorem was presented for identifying the degree of freedom of power systems, and the number of power processors required for regulating its operation point. The conclusion in [31] is that the degree of freedom of a system's operation point must be equal to the number of power processors (converters) used to control it. Applying this theorem to the DMPPT architectures gives rise to the following guideline:

Lemma 1 *A system with N photovoltaic modules must contain N Maximum Power Point trackers in order to facilitate global MPPT.*

An MPP tracker is any unit that actively optimizes power. It may or may not include an inner closed loop regulator, and can be situated either in the embedded MICs

or in a central (string) inverter. If less than N MPPT units are used, the operation point cannot be set to harvest maximum power. If more than N MPPT units are used, the control structure is redundant and might go unstable. The location of the MPPT units in the front-end DC optimizers' architecture is shown in Fig. 8. The system contains N photovoltaic modules, therefore should contain N MPPT units, including the one of the inverter. Thus, according to Lemma 1, the inverter must not contain an MPPT unit, as this additional MPPT unit in the inverter may invoke instabilities or maximum power search dead-locks. The correct control structure is shown in Fig. 8(a). The MPPT units are applied in the MICs and the inverter applies only a closed loop feedback that regulates the string's voltage. Figure 8(b) shows a redundant control structure, including the unnecessary inverter MPPT unit. The inverter's MPPT is redundant because the power injected to the DC bus is regulated independently by the MICs. The MICs keep the PV modules operation at maximum power, while adjusting their voltage gains to match the string's bus voltage. The MICs outputs may be regarded as power sources, thus with any bus voltage, within a certain limit, maximum power is extracted towards the DC buss. Since the power injected to the bus is constant, the inverter should only regulate the bus voltage. It does so by means of a simple closed loop regulator. If the inverter would feature an MPPT unit at its front end, instead of a closed loop regulator, the overall maximum power search process may enter a deadlock or even become unstable because the additional inverter's MPPT may attempt to shift the bus voltage without affecting the string output power. This is why operating conventional string inverters with a DMPPT system may be problematic. Most string inverters are designed to operate with conventional photovoltaic arrays (with no embedded MICs), thus they include an MPPT unit. This unit might destabilize the MICs within the DMPPT architecture.

In order to demonstrate the instability of a system with the supplementary MPPT unit, we simulate the DMPPT architecture in two modes of operation: In the first mode, the inverter is controlled by a negative feedback loop that regulates the bus voltage. In the second mode, the inverter is controlled by an MPPT unit that adjusts the bus voltage in search of the maximum power point. Simulation results are shown in Fig. 9, and the various simulation parameters are detailed in Table 1.

Throughout this simulation, the MICs and the inverter are treated as ideal power processors, with 100% efficiency, infinite bandwidth, and zero input and output ripples. These assumptions enabled us to simplify the simulation models and to demonstrate the essential instability associated with the $N + 1$ MPPT structure. The MICs are modeled by controlled current sources at their inputs and controlled voltage sources at their outputs. The input voltage is controlled by a local MPPT unit, and the output voltage is set so that the output power equals the input power. The local DC-DC MPPT is based on the 'perturb & observer' (P&O) algorithm. It samples the PV voltage and current and alters the PV voltage to iteratively maximize the power. The inverter's control is composed of three cascaded loops. The inner most loop is the current loop that regulates the inductor's current, i_g, to a target signal i_g^*. In simulation, this loop is considered ideal, so it is assumed that $i_g = i_g^*$ at any given instant. The target current, i_g^*, is set to be instantaneously proportional to the grid voltage v_g by means of a multiplier. This drives a sinusoidal current in-phase with the voltage (in some similarity to active power factor rectification). The amplitude of current, $I_{g,m}^*$ is set by the voltage loop negative feedback. As the input voltage increases, the amplitude of current follows the increase in order to moderate the voltage. The voltage loop compensator consists of two stages: A three pole Butterworth filter, in order to filter out the 100Hz voltage ripple induced in the dc-link capacitor, and a proportional-integral-derivative (PID) controller, which is much slower than the grid's frequency (50Hz). The input bus voltage is regulated according to the target signal V_{string}^*. The source

Table 1. DMPPT simulation parameters

Parameters	Values	
Photovoltaic modules		
Isolation	1.0	sun
Maximum power	54.8	W
Voltage at maximum power	20.0	V
Current at maximum power	2.74	A
Number of modules in series	10	-
DC-DC converters		
Efficiency	100	%
MPPT voltage step	0.1	V
MPPT step time	100	ms
Inverter		
Efficiency	100	%
Grid voltage	220	V_{RMS}
Grid frequency	50	Hz
Voltage-bus capacitor (*Cbus*)	200	µF
bus-voltage target (*Vstring**)	350	V
MPPT voltage step	1	V
MPPT step time	100	ms
Inverter's voltage loop PID controller		
Proportional constant	0.01	-
Integral constant	0.1	-
Derivative constant	0	-
Inverter's voltage loop Butterworth filter		
Number of poles	3	-
Cut-off frequency	10	Hz

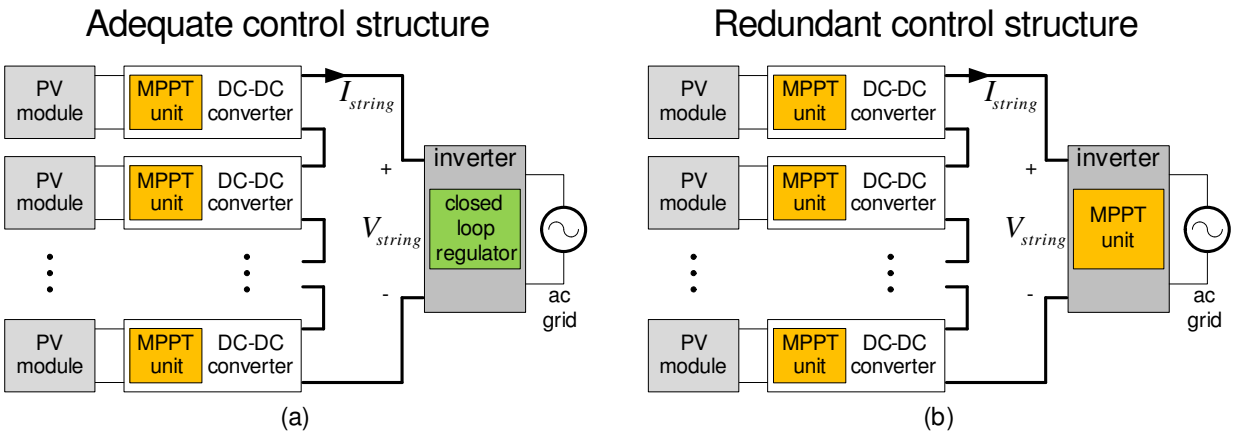

Fig. 8. Position of the MPPT units in the front-end DC optimizers' architecture (a) adequate control structure with N MPPT units, (b) redundant control structure with $N+1$ MPPT units

of this signal depends on the mode of operation. If the inverter is controlled by a simple closed-loop regulator, V^*_{string} is a constant (350V in this simulation example).

If the inverter is controlled by the MPPT unit, this unit samples the bus voltage and current and alters the target voltage, V^*_{string}, in an attempt to maximize the string's output power.

Figure 9(b) shows simulation results when the inverter is controlled in a closed loop, regulating the string voltage to a constant 350V. The system is seen to be stable and maximum power is extracted towards the grid. Figure 9(c) shows results in the case in which the inverter contains an MPPT unit. The resulting amplitude of current is almost identical to the regulated case, so the system successfully transfers the full power to the grid. However, the bus voltage is evidently unstable demonstrating a swing of about 150V.

This swing is generated due to the operation of the inverter's MPPT. The MPPT unit senses the power injected to the bus and alters the bus voltage in order to maximize the power. However, the power is already maximized due to the MICs operation, so the MPPT 'sees' no change and the search process diverges over time.

5 MINIMAL-POWER PROCESSING ARCHITECTURES

'Minimal power processing' architectures applies a small fraction of the generated power in order to balance the string operation point [20 - 25]. The concept behind these architectures is to auxiliary process small amounts of power to balance the generated current of shaded PV modules in order to facilitate maximization of the total generated power. This is accomplished by a DC-DC converter that is connected in parallel to each module. The minimal power processing architectures feature the advantage of processing only a small fraction of generated power, in contrast to the front-end DC optimizers which process the full generated power. Typically, the power processed by the DC-DC converters is small, thus losses are minimized and the efficiency is high (this resembles the power flow in autotransformers which also exhibit efficiencies that are higher than those of regular transformers).

Three types of architectures are presented in Fig. 10. They differ by the source of auxiliary power, i.e. the DC-DC converters input. With the shuffling architecture (Fig. 10(a)) [7, 20], a DC-DC converter interconnects each pair of adjacent modules, and can 'shuffle' power between illuminated modules and shaded ones to eliminate possible mismatch.

An example of string equalization by means of the shuffling architecture and the resulting flow of power is illustrated in Fig. 11(a), where two PV modules are matched to a string current of 2 A. In this example, the converter draws 0.2 A from the highly insolated module, and injects 0.1 A across the shaded module, thus restoring the symmetry of the string. For the shuffling architecture, the DC-DC converters' must invert the voltage polarity. Isolation by a transformer is not necessary as the ground of the converter is common to both PV modules, however, the power stage should enable bidirectional power flow and thus it must employ a bidirectional synchronous switch (the secondary switch must be realized by a MOSFET rather than a diode). Several standard power topologies are suitable, such as the inverting buck-boost converter, or the C'uk converter [7, 20].

In [21] and [22], Shimizu el al. proposed the Generation Control Circuit, where the currents of modules within a

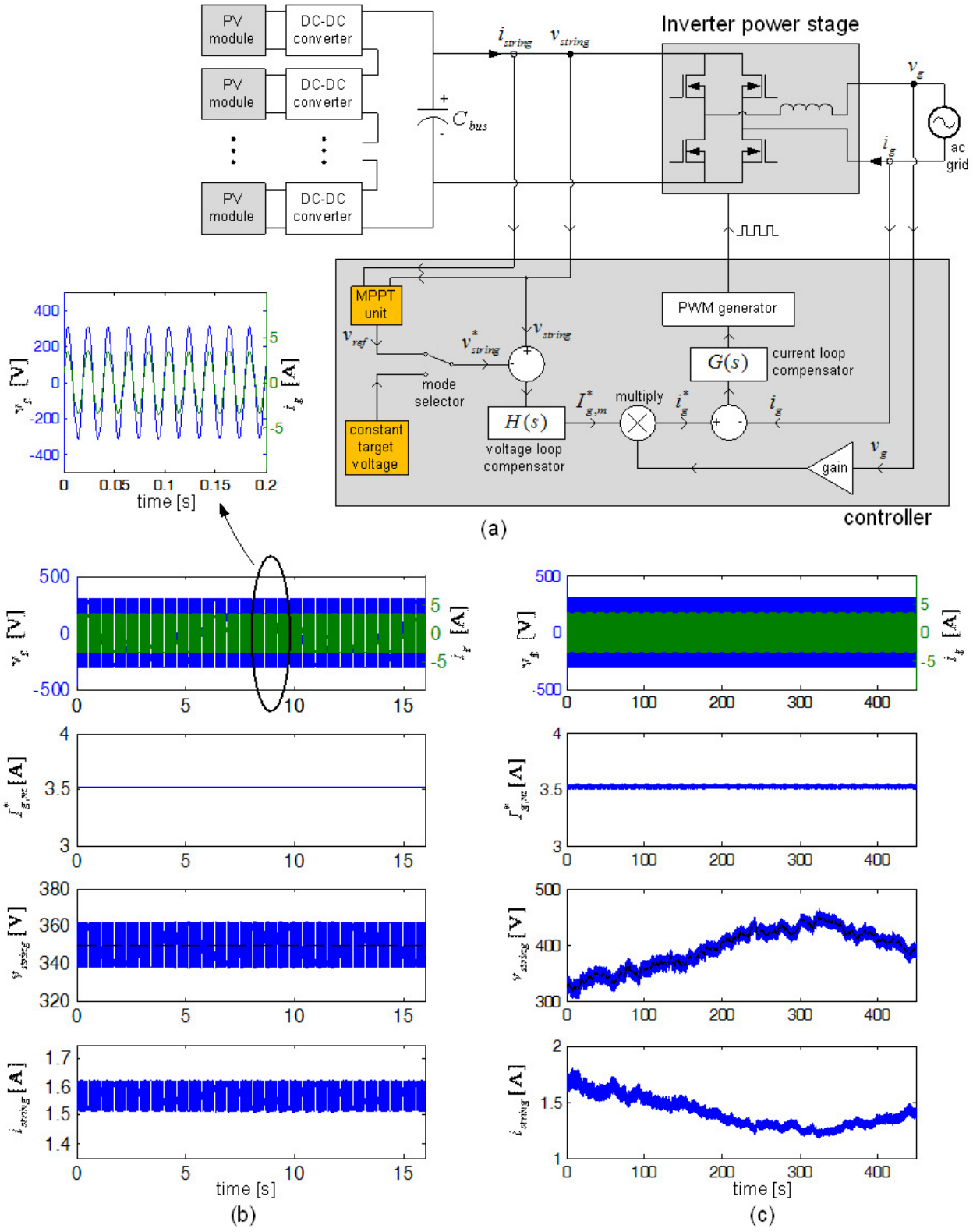

Fig. 9. Simulation for a DMPPT architecture including a string inverter (a) system structure and control loop, (b) steady-state simulation, when the string voltage is regulated to be constant, and (c) steady-state simulation, when the inverter is controlled by an MPPT unit, exhibiting string-voltage instability

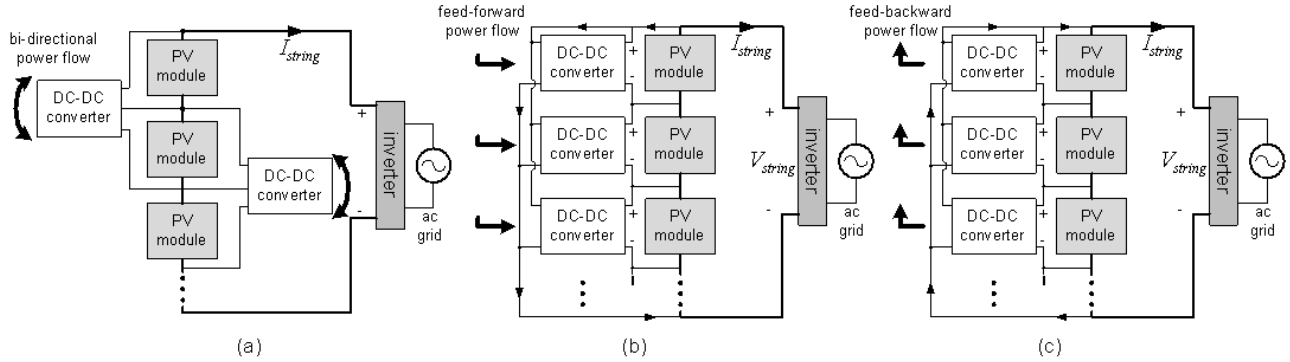

Fig. 10. Minimal power-processing architectures (a) shuffling converters, (b) returned energy current converters (RECC) with feed-back power flow, and (c) feed-forward current converters

string are decoupled, thereby facilitating operation of each module at its MPP. However, it was realized in [23] that, due to the internal bypass diodes (in shunt with substrings of PV cells), mismatch may yet occur even within individual modules; thus, active voltage sharing between two substrings of an individual module by means of a buck-boost converter was proposed. Optimization of the active bypass converter of [23] was reported in [24], where it was concluded that, in terms of efficiency, the bypass structure is very competitive with respect to boost, buck or buck-boost based solutions.

The Returned Energy Current Converters' (RECC) based architecture [25] is shown in Fig. 10(b). It applies shunt DC-DC converters to balance the shaded modules by injecting a compensation current in parallel with the modules, thus equalizing their photonic generated current to the string current. The power associated with this current injection is fed to the converters' inputs from the overall string (the dc link capacitor).

Energy Feed Forward architecture is depicted in Fig. 10(c). In this architecture the string equalization is attained by diverting part of the excess current from higher insolated modules through the shunt converters, thus evacuating part of the module's power through the converter. Thus, in both cases, DC-DC converters that are connected in parallel with the modules balance the string.

The feed-back architecture draws current from the DC bus, and injects it across shaded modules, compensating for its missing current. The string current is equalized to that of the most energetic module. In contrast, the feed-forward architecture extracts current from more energetic modules and injects it directly to the DC bus. In this case, the string current is equalized to the current of the least energetic module.

The power flow of the feed-back architecture is demonstrated in Fig. 11(b), where a shaded module is matched to a string current of 2 A. The parallel converter draws power from the DC bus and injects 0.3 A to compensate the module's generated current of 1.7 A.

Many standard isolating topologies may be used. Typical candidates are the flyback, forward, and half-bridge topologies.

Figure 12 shows a comparison of the overall system efficiency for the front-end converters based architecture and the RECC architecture. Figure 12(a) shows the conversion efficiency against the average shading level, assuming a constant converters' efficiency of 0.9. In Fig. 12(b) the converters' efficiency is varied while an average shading level of 20% is kept constant. The increase in conversion efficiency, thanks to the shunt current compensation, is notable.

This is due to the much reduced auxiliary processed power (the power flowing through the DC-DC converters) with respect to the front-end DMPPT. For instance, if there is no shading (uniform illumination) the processed power is zero and the system's efficiency is 1.

As the average shading increases, the currents injected to the PV modules must also increase in order to compensate for the scatter of the photon generated currents. As a result, the power processed by the converters increases, reducing the conversion efficiency. In contrast, with the front-end converters, the efficiency is constant and equal to the efficiency of converters over all shading levels.

5.1 Control of Minimal Power Processing Architectures

The control of minimal power processing architectures is challenging because the PV modules are not decoupled from each other, so variations of the operation point of one module may affect the entire string. The MPPT algorithms must account for these mutual dependencies otherwise the operation points might diverge, or enter a dead-lock around a spurious maximum power point. We

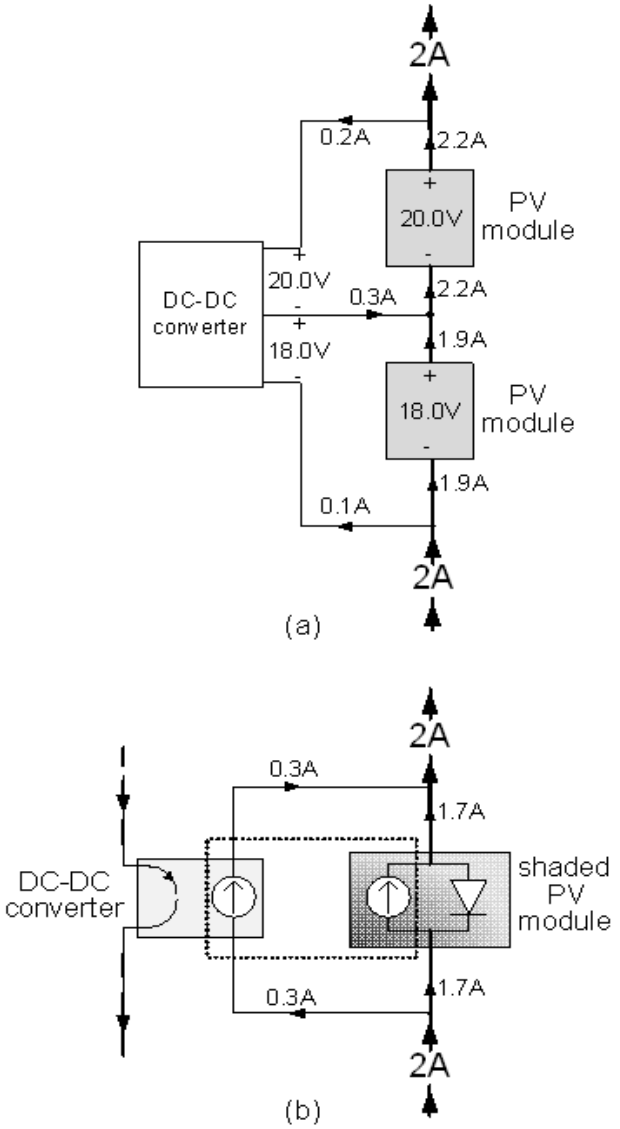

Fig. 11. Minimal power-processing based string equalization example (a) shuffling converter, (b) RECC

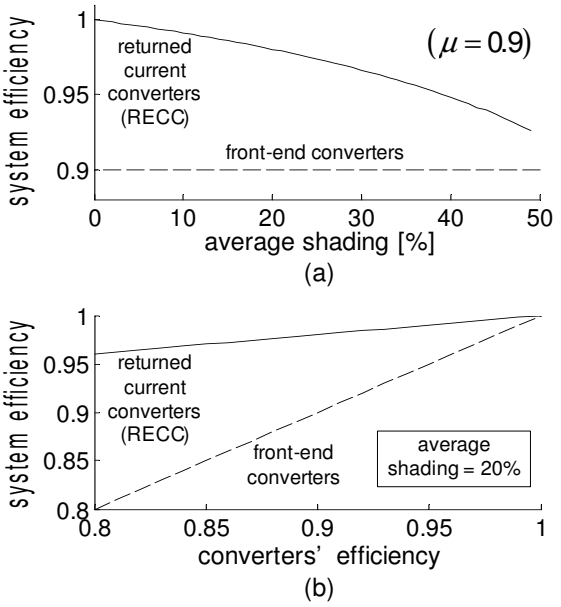

Fig. 12. Efficiency comparison: front-end converters versus RECC architectures (a) converters' efficiency is assumed constant at 0.9, (b) average shading is constant at 20%

believe that these questions are interesting for future research. However, in the following section we just examine the location of MPPT units within these architectures, ignoring the stability issues.

The location of MPPT units must follow the guideline presented in Lemma 1: A system with N photovoltaic modules must contain exactly N Maximum Power Point tracking (MPPT) units. This principle is not intuitive with these architectures, as seen in Fig. 13, showing MPPT locations for a string of $N = 3$ modules.

As a general rule, with these architectures, the inverter MUST contain an MPPT unit, as a simple closed loop regulator is not sufficient in order to extract maximum power.

The power output of the string, including the auxiliary converters, is predetermined by the maximum power point of the PV modules, as all generated power must flow to the load. The bus voltage is also predetermined (it must be equal to the sum of the PV modules voltages at maximum power point). Therefore, at the output of the string (at the input of the inverter) both power and voltage are predetermined by the maximum power point of the modules. As a result, the string's output current is also fixed, as it must be equal to the division of power by voltage. These principles are expressed by (3), which holds for all minimal power processing architectures. Since the string's voltage and current at the MPP are determined by the DC side (string of modules + balancing converters), the inverter input must be matched in order to allow operation with both these values (V_{string}, I_{string}).

$$\begin{aligned} P_{string} &= \sum_i V_{mpp,i} \cdot I_{mpp,i} \\ V_{string} &= \sum_i V_{mpp,i} \\ I_{string} &= \frac{P_{string}}{V_{string}} \end{aligned} \tag{3}$$

In other words, the inverter's input must present an equivalent impedance of:

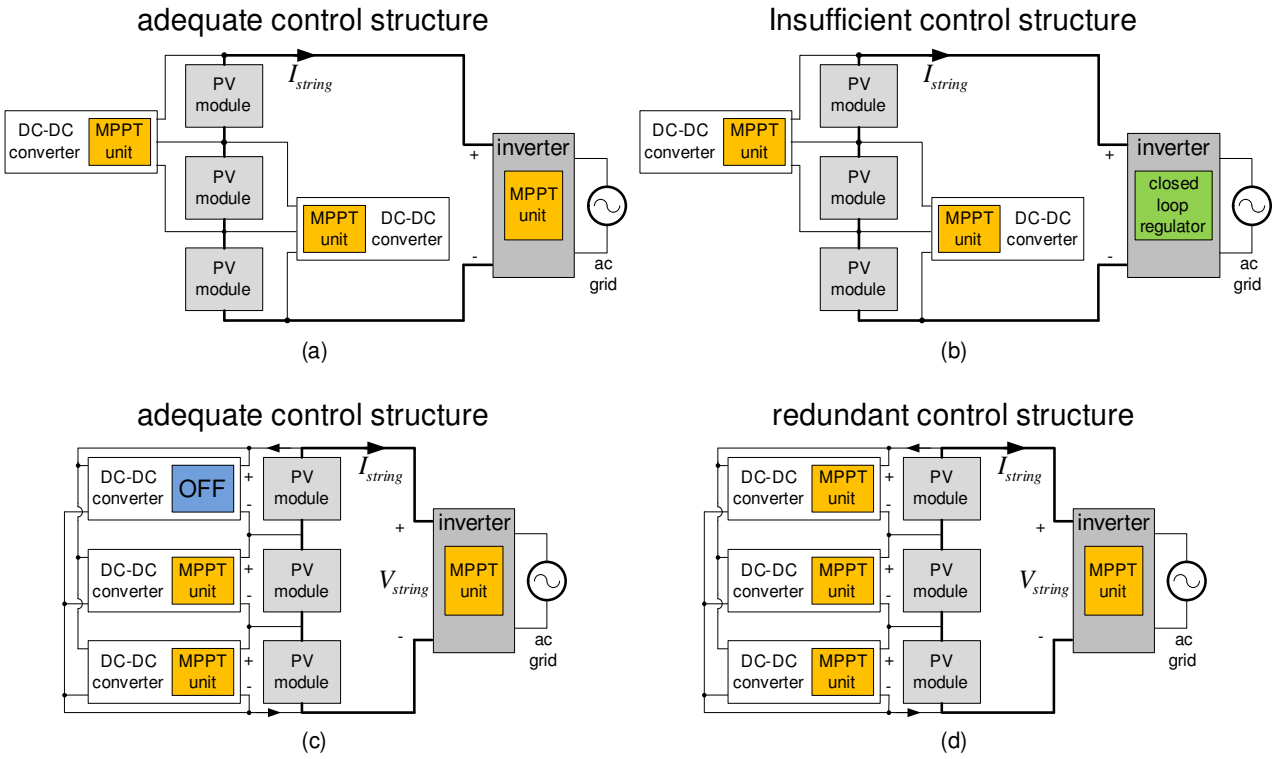

Fig. 13. Location of the MPPT units in some minimal power-processing architectures (for a string of $N = 3$ modules) (a) shuffling adequate control with 3 MPPT units, (b) shuffling insufficient control with 2 MPPT units, (c) RECC adequate control with 3 MPPT units, and (d) RECC redundant control with 4 MPPT units

$$Z_{inv} = \frac{V_{string}}{I_{string}} \tag{4}$$

Therefore, regulating the inverter by means of a negative feedback control loop will reduce the harvested power. Thus, the inverter must contain an active MPPT unit that tracks the optimal operation point of the string.

For this reason, minimal power processing topologies may operate with standard string or array inverters which already contain an embedded MPPT controller.

Because the total number of MPPT units must equal the number of PV modules, and since the inverter must contain one unit, the string must be operated with $N - 1$ MPPT units. Operating it with N MPPT units is redundant and may invoke instabilities or deadlocks. This is demonstrated in Fig. 13. In module (b) the inverter is controlled by a closed loop regulator, a structure which is insufficient to extract maximum power. Modules (a) and (c), where two active MPPT units are embedded in the string, show adequate control structures. The shuffling method is presented in (a). It includes two DC-DC converters, each with a MPPT unit. The returned current method is presented in (c). Here, three DC-DC converters are used, but according to our analysis, one of them must be turned off, otherwise it will destabilize the string. This redundancy is demonstrated in module (d).

6 CONCLUSIONS

This work presents high-level architectural aspects of photovoltaic DMPPT systems and their performance in terms of efficiency, control and stability. PV string operation under inhomogeneous insolation is clarified. In addition, a distinction between feedback based regulation and MPPT is emphasized. MPPT units' location is discussed and possible instabilities are demonstrated.

The architectures are classified in two categories: the full power processing category, of which mainly the front-end DC optimizers architecture is analyzed, and the minimal power processing category, consisting of the shuffling, the RECC, and the Energy Feed Forward architectures.

We discuss the pros and cons of the various architectures. Front-end DC optimizers are capable of decoupling the PV modules from the string, while maximizing the output power of each module. This architecture is simple to control, low cost, efficient and robust. However, it processes the full power generated by the PV string, and suf-

fers the consequential losses. On the other hand, equalization methods imply minimal auxiliary power-processing; only the imbalance power is processed.

By equalizing the string and restoring the symmetry, the maximum potential power may be extracted. As a result, equalization methods exhibit a higher overall efficiency. However, with these structures the modules are not decoupled from the string, which make the control more complex.

The location of MPPT units within DMPPT architectures is analyzed, applying a simple guideline: A system with N photovoltaic modules must contain exactly N MPPT units. This principle is shown to impose constraints on the location of MPPT units within power architectures. If more than N MPPT units are applied, then the maximum power search algorithm might go unstable. Such instability is demonstrated by simulation in Fig. 9(c).

REFERENCES

[1] S. Poshtkouhi, J. Varley, R. Popuri, and O. Trescases, "Analysis of distributed peak power tracking in photovoltaic systems," *IEEE International Power Electronics Conference*, 2010, pp. 942 –947.

[2] J. Myrzik and M. Calais, "String and module integrated inverters for single-phase grid connected photovoltaic systems - a review," in *Power Tech Conference Proceedings, 2003 IEEE Bologna*, vol. 2, June 2003, pp.1–8.

[3] R. Erickson and A. Rogers, "A microinverter for building-integrated photovoltaics," in *Applied Power Electronics Conference and Exposition, 2009. APEC 2009. Twenty-Fourth Annual IEEE*, Feb. 2009, pp. 911–917.

[4] G.R Walker and P.C Sernia, "Cascaded DC–DC converter connection of photovoltaic modules," IEEE 33rd Annual Power Electronics Specialists Conference, PESC 02, 2002 pp. 24–29.

[5] G.R Walker and P.C Sernia, "Cascaded DC–DC converter connection of photovoltaic modules," IEEE Transactions on Power Electronics, vol. 19, no. 4, 2004, pp. 1130–1139.

[6] N. Femia, G. Lisi, G. Petrone, G. Spagnuolo and M. Vitelli, "Distributed maximum power point tracking of photovoltaic arrays: Novel approach and system analysis," *Industrial Electronics, IEEE Transactions on*, vol. 55, no. 7, Jul. 2008, pp. 2610–2621.

[7] G.R. Walker, *J.* Pierce, *"*PhotoVoltaic DC-DC Module Integrated *C*onverter for Novel Cascaded and Bypass Grid Connection Topologies — Design and Optimisation*," IEEE* Power Electronics Specialists Conference, 2006. PESC '06. *pp. 1-7.*

[8] Poshtkouhi, S.; Palaniappan, V.; Fard, M.; Trescases, O.; , "A General Approach for Quantifying the Benefit of Distributed Power Electronics for Fine Grained MPPT in Photovoltaic Applications using 3D Modeling," *Power Electronics, IEEE Transactions on*, vol.PP, no.99, pp.1, 0

[9] E. Duran, M. Sidrach-de-Cardona, J. Galan, J.M. Andujar, "comparative analysis of buck-boost converters used to obtain I-V characteristic curves of photovoltaic modules.", *IEEE Power Electronics Specialists Conference, 2008.* (PESC 2008), pp. 2036-2042.

[10] L. Linares, R.W. Erickson, S. MacAlpine and M. Brandemuehl, "Improved Energy Capture in Series String Photovoltaics via Smart Distributed Power Electronics," *Twenty-Fourth Annual IEEE Applied Power Electronics Conference and Exposition, 2009,* (APEC 2009), pp. 904–910.

[11] R.K. Hester, C. Thornton, S. Dhople, Z. Zheng, N. Sridhar, D. Freeman, "High efficiency wide load range buck / boost / bridge photovoltaic microconverter", *Twenty-Sixth Annual IEEE Applied Power Electronics Conference and Exposition, 2011.* (APEC 2011), pp. 309 - 313.

[12] R. Kadri, J.P. Gaubert, G. Champenois, "Non-dissipative String Current Diverter for Solving the Cascaded DC-DC Converter Connection Problem in Photovoltaic Power Generation System," *Power Electronics, IEEE Transactions on* , vol.PP, no.99, pp.1, 0.

[13] H. Valderrama-Blavi, C. Alonso, L. Martinez-Salamero, S. Singer, B. Estibals and J. Maixe-Altes, "AC-LFR concept applied to modular photovoltaic power conversion chains," *IEE Proc. Electric Power Applications*, vol. 149, no. 6, Nov. 2002, pp. 441–448.

[14] Bangyin Liu; Chaohui Liang; Shanxu Duan; , "Design considerations and topology selection for dc-module-based building integrated photovoltaic system," *Industrial Electronics and Applications, 2008. ICIEA 2008. 3rd IEEE Conference on* , vol., no., pp.1066-1070, 3-5 June 2008.

[15] L. Bangyin, D. Shanxu, C. Tao, "Photovoltaic DC-Building-Module-Based BIPV System—Concept and Design Considerations," *Power Electronics, IEEE Transactions on*, vol.26, no.5, pp.1418-1429, May 2011.

[16] G. Velasco-Quesada, F. Guinjoan-Gispert, R. Pique-Lopez, M. Roman-Lumbreras and A. Conesa-Roca, "Electrical PV Array Reconfiguration Strategy for Energy Extraction Improvement in Grid-Connected PV Systems," *IEEE Tran. on Industrial Electronics*, vol. 56, no. 11, Nov. 2009, pp. 4319–4331.

[17] L. Yanli, P. Zhichao, C. Ze, "Research on an adaptive solar photovoltaic array using shading degree model-based reconfiguration algorithm," *Control and Decision Conference (CCDC), 2010 Chinese* , vol., no., pp.2356-2360, 26-28 May 2010.

[18] V. d'Alessandro, S. Daliento, P. Guerriero, M. Gargiulo, "A novel low-power active bypass approach for photovoltaic panels," *Clean Electrical Power (ICCEP), 2011 International Conference on*, vol., no., pp.89-93, 14-16 June 2011.

[19] G. Acciari, D. Graci, A. La Scala, "Higher PV Module Efficiency by a Novel CBS Bypass," *Power Electronics, IEEE Transactions on*, vol.26, no.5, pp.1333-1336, May 2011.

[20] G.R. Walker, J.K. Xue, and P.C. Sernia, “PV string per-module maximum power point enabling converters,” *Proceedings of the Australasian Universities Power Engineering Conference, Christchurch,New Zealand, 28 September–1 October, 2003*. pp. 112–117.

[21] T. Shimizu, M. Hirakata, T. Kamezawa and H. Watanabe, "Generation control circuit for photovoltaic modules," *Power Electronics, IEEE Transactions on,* vol. 16, pp. 293-300, 2001.

[22] T. Shimizu, O. Hashimoto and G. Kimura, "A novel high-performance utility-interactive photovoltaic inverter system,"*Power Electronics, IEEE Transactions on,*vol. 18, pp. 704-711, 2003.

[23] R. Giral, C.A. Ramos-Paja, D. Gonzalez, J. Calvente, A. Cid-Pastor and L. Martinez-Salamero, “Minimizing the effects of shadowing in a PV module by means of active voltage sharing,” *2010 IEEE International Conference on Industrial Technology (ICIT),* 2010, pp. 943–948.

[24] R. Giral, C. E. Carrejo, M. Vermeersh, A. J. Saavedra-Montes and C. A. Ramos-Paja, "PV field distributed maximum power point tracking by means of an active bypass converter," in *Clean Electrical Power (ICCEP), 2011 International Conference on,* 2011, pp. 94-98.

[25] Y. Nimni and D. Shmilovitz, “A Returned Energy Architecture for Improved Photovoltaic Systems Efficiency,” *IEEE International Symposium on Circuits and Systems,* Paris (ISCAS 2010), May 2010, pp. 2191–2194.

[26] K.H. Hussein, I. Muta, T. Hoshino, M. Osakada, “Maximum photovoltaic power tracking: an algorithm for rapidly changing atmospheric conditions,” *IEE Proc. Generation Transmission and Distribution,* 1995, 142, pp. 59–64.

[27] P. Maffezzoni, D. D’Amore, “Compact Electrothermal Macromodeling of Photovoltaic Modules,” *IEEE Trans. on Circuits and Systems II*, vol. 56, no. 2, February 2009, pp. 162–166.

[28] R. Paul, D. Maksimovic, "Analysis of PWM nonlinearity in non-inverting buck-boost power converters", *IEEE Power Electronics Specialists Conference, 2008*, (PESC 2008), pp. 3741 - 3747.

[29] L. Young-Joo, A. Khaligh, A. Emadi, "A compensation technique for smooth transitions in non-inverting buck-boost converter", *Twenty-Fourth Annual IEEE Applied Power Electronics Conference and Exposition, 2009*. (APEC 2009), pp. 608-614.

[30] D. Shmilovitz, Y. Levron, "Sliding mode control of photovoltaic module integrated buck-boost converters," in *Power Electronics and Motion Control Conference (EPE/PEMC), 15th International,* 2012, pp. 1-5.

[31] S. Singer, "Canonical approach to energy processing network synthesis", *IEEE Transactions on Circuits and Systems*, Vol. 33, Aug 1986 pp. 767 – 774.

Doron Shmilovitz (M’98) received his BSc, MSc, and PhD from Tel-Aviv University, Tel-Aviv, Israel, in 1986, 1993, and 1997, respectively, all in electrical engineering. During 1986–1990 he worked in R&D for the IAF, where he developed programmable electronic loads. During 1997–1999, he was a Post-Doctorate Fellow at the New York Polytechnic University, Brooklyn. Since 2000, he has been with the Faculty of Engineering, Tel-Aviv University. His research interests include switched-mode converters, topology, dynamics and control, and circuits for alternative energy sources and for powering of sensor networks and implanted medical devices, and general circuit theory.

Yoash Levron received his BSc from the Technion, Haifa, Israel, and an MSc from the Tel-Aviv University, Israel, in 2001 and 2006, respectively. He is currently pursuing his PhD at Tel-Aviv University. His research focuses on the control of power processing systems.

AUTHORS’ ADDRESSES

Assoc. Prof. Doron Shmilovitz, Ph.D.
Yoash Levron, M.Sc.
Department of Physical Electronics,
Faculty of Engineering,
Tel-Aviv University,
Ramat Aviv, 69978, Tel-Aviv, Israel
email: shmilo@post.tau.ac.il, yoashlevron@gmail.com

Received: 2012-01-30
Accepted: 2012-04-04